

# **Tribological Behavior of Aluminium Metal Matrix Composite with Addition of Bamboo Leaf Ash by GRA-Taguchi Method**

B.P. Kumar<sup>a</sup>, A.K. Birru<sup>a</sup>

<sup>a</sup>Department of Mechanical Engineering, National Institute of Technology Manipur, Imphal, Manipur, India.

## **Keywords:**

Aluminium composite  
Bamboo leaf ash  
Stir casting  
Dry sliding wear  
Grey relational analysis  
SEM analysis

## **ABSTRACT**

The bamboo leaf ash (BLA) which was extruded from agro waste was used as a particulate reinforcement to produce economical AMMCs. The dry sliding wear behavior of Al-4.5 wt.% Cu alloy with the addition of 2, 4 and 6 wt.% of BLA by stir casting method was analyzed using pin-on-disc wear test apparatus. The typical  $L_{27}$  orthogonal array was selected to perform the experimental work. The effect of the testing parameters on wear rate, SWR and COF of the fabricated aluminium composites were studied using Grey relational analysis with Taguchi method. The ANOVA analysis was employed to identify the significance of testing parameters and statistical analysis was performed. The testing parameters play a crucial role to control the dry sliding wear behavior of the fabricated aluminium composites. The confirmation test has been performed to validate the predictive statistical value with the experimental value. The wear mechanism was analyzed using scanning electron microscope with Energy Dispersive Analysis of X-ray, it was observed that the grooves size decreased with the addition of BLA particles in the composite in comparison with matrix alloy resulting in decreased wear rate with increase in BLA content. The significant amount of mechanical mixed layer formation was observed to increase in wear resistance of the composites.

## **Corresponding author:**

Anil Kumar Birru  
National Institute of Technology  
Manipur, Imphal, Manipur,  
India – 795004.  
Email: anilbirru@gmail.com,

© 2018 Published by Faculty of Engineering

## **1. INTRODUCTION**

Aluminium alloys have raised considerable interest in recent years due to the fact that they have good strength to weight ratio, stiffness, and wear resistance and can be used as structural and also bearing materials [1]. The desirable properties of aluminium alloys may be improved by alloying [2], heat treatment [3], and dispersion strengthening [4]. The dispersion

strengthening is achieved by dispersion of reinforcement particles in the aluminium matrix alloy and is widely accepted [5]. The particles reinforced aluminium is known as Aluminium Metal Matrix Composites (AMMCs). The incorporation of the reinforced particles in the AMMCs strengthen the tribological properties and the acquired composites can replace monolithic materials for various engineering applications such as automobile, aerospace,

marine industries [6]. AMMC is an acceptable method to enhance the wear resistance of aluminium alloys and typically, numerous types of ceramic particles such as SiC [7], Al<sub>2</sub>O<sub>3</sub> [8], TiC [9], TiB<sub>2</sub> [10], and WC [11] are used as reinforcements for AMMCs.

Moses and Joseph [12] studied dry sliding wear behavior of AA6061 matrix alloy reinforced with various weight percent of SiC particles by stir casting method. It was suggested that the wear rate of the matrix alloy was minimized with addition of SiC content. Suresh et al. [13] reported that with the addition of TiB<sub>2</sub> in the Al6061 matrix alloy, tensile strength and wear resistance enhanced significantly in comparison with matrix alloy. It is observed that from the previous researcher's work that the reinforcements used were relatively expensive and not readily available in most of the developing countries. The fabrication cost of AMMCs may be reduced by using potential industrial and agricultural waste debris such as Fly Ash, Bagasse Ash, Rice Husk Ash (RHA), Coconut shell ash, Bamboo Leaf Ash (BLA) etc as a reinforcement material [14,15]. Apasi et al. [16] studied wear behaviour of Al-Si-Fe alloy with the addition of coconut shell ash by stir casting method, the hardness and wear resistance were remarkably increased over the matrix alloy. Saravanan et al. [17] fabricated AlSi10Mg-RHA composite with various size of RHA particles by stir casting method and it was suggested that the wear rate was reduced with an increase in the size of RHA particles. Furthermore, Baburao et al. [18] analyzed dry sliding wear behavior of the aluminium composite with the addition of fly ash particles by stir casting method and it was concluded that the wear rate was minimized with increase in fly ash content in the composite. This was due to formation of a mechanically mixed layer (MML) which reduced contact between the matrix and reinforcement particles.

The dry sliding wear behavior is affected by various testing parameters and the relation between the parameters, and wear behavior is complicated and interconnected. The optimal condition of the testing parameters is important for dry sliding wear behavior. The Taguchi method is used for optimization of multivariable to the single response by earlier researchers. Senthilkumar et al. [19] observed that the testing parameters such as applied load (AL) and weight

percent of RHA, and also sliding velocity (SV) were influenced significantly on wear behavior of AlSi10Mg-RHA composites by Taguchi and ANOVA analysis. Optimization of multiple responses is much more complex than single response characteristic. The Taguchi method coalesced with Grey Relational Analysis (GRA) to solve the optimization of multiple response characteristics of dry sliding wear behavior. Dharmalingam et al. [20] examined the dry sliding wear behavior of AlSi10Mg-Al<sub>2</sub>O<sub>3</sub>-MoS<sub>2</sub> hybrid composite with the Grey-Taguchi method. It was noted that the optimum level of specific wear rate (SWR) and coefficient of friction (COF) for multivariable such as MoS<sub>2</sub> weight percent followed by SV and AL parameters were influenced significantly. Rajesh et al. [21] analysed the SWR and COF of reinforced aluminium composites with addition red mud. The optimization was performed by using Taguchi method linked with GRA and from the result it was concluded that the red mud and sliding velocity were the critical parameters among the testing parameters that affected the SWR and COF, followed by the counterpart material hardness and applied load. Rajesh et al. [22] also analyzed the tribological behavior of Al-SiC composites with the Grey-Taguchi method.

The BLA is a most economical and has lower density and available in large quantities as an agro waste among numerous variety of reinforcement material [23]. The fabrication expenses may be overcome for wide applications in automotive and aerospace industries with BLA as reinforcement in the aluminium composites. The present research work has been carried out with the utilization of BLA as reinforcement. It is available a large quantity as an agricultural waste in North East region India, and incorporating into aluminium matrix to produce aluminium metal matrix composites with stir casting method. The significance of BLA particles on the dry sliding wear behavior at room temperature of Al-4.5 wt.% Cu alloy using GRA and Taguchi method was studied. The standard L<sub>27</sub> orthogonal array and GRA are unified to study the experimental outcomes of dry sliding wear performance from 27 trials by changing the testing parameters such as applied load (AL), sliding velocity (SV) and the weight percentage of BLA (BL). This analysis was done for the Al-4.5Cu alloy addition with 2, 4 and 6 wt.% of BLA particles

respectively. The optimum combinations of testing parameters were observed. The effect of each parameter and their interactions on the dry sliding wear behavior was analyzed by Analysis of Variance (ANOVA).

## 2. MATERIALS AND EXPERIMENTAL DETAILS

The Al-4.5 wt.% Cu alloy with density 2.7876 g/cm<sup>3</sup> was selected as a matrix alloy for the present research work and chemical compositions were shown in Table 1. Bamboo leaf ash was extruded from agro waste, with an average particle size 75 µm and an average density 1.81 g/cm<sup>3</sup> has been selected as a reinforcement material and chemical compositions were shown in Table 2. Magnesium in ingot form was used to enhance the wettability among the matrix alloy and BLA particles during the processing of the aluminium composites. The aluminium composites with addition at 2, 4 and 6 wt.% of BLA fabricated by stir casting method. It is moderately economical method and offers a wide assortment of materials and fabrication conditions, and it exhibits good bonding between matrix and reinforcement particles due to stirring action of reinforcement particles into the melts [24]. The BLA particles were preheated at a temperature of 600 °C to remove the dampness and to improve the wettability with matrix alloy. The Al-4.5 wt.% Cu matrix alloy was heated up to 800 °C using electric resistance furnace. The liquid metal was then cooled below the liquid state (about 620-650 °C) to maintain semisolid state. The preheated BLA particles were incorporated and mixed manually. Manual mixing was carried out as it was very hard to mix with automatic mechanical stirrer in a semisolid state. The aluminium composite melt was then superheated at 750 ±10 °C to reach fully liquid state, and mechanical mixing was performed for about 10 minutes. After thorough stirring, the melt was poured into steel mould which was preheated at 350 °C and allowed to cool to obtain aluminium composites cast rods.

**Table 1.** Chemical composition of Al-4.5 wt.% Cu alloy.

Element	wt.%	Element	wt.%	Element	wt.%
Cu	4.52	Mn	0.131	Sn	0.021
Fe	0.663	Ni	0.075	Ti	0.013
Si	0.538	Mg	0.066	Al	Balance
Zn	0.118	Pb	0.029		

**Table 2.** Chemical compositions of Bamboo Leaf Ash.

Element	SiO <sub>2</sub>	CaO	K <sub>2</sub> O	C	Al <sub>2</sub> O <sub>3</sub>	MgO	Fe <sub>2</sub> O <sub>3</sub>
wt. %	76.2	6.68	5.62	4.2	4.13	1.85	1.32

The samples of the fabricated composites were sectioned for microstructure examination. The metallographic examination of the fabricated aluminium composites was carried out using an optical microscope (OM) and Scanning Electron Microscopy (SEM) for distribution of reinforcement particles. The density of all the composites was measured by water displacement technique (Archimedes' principle) [25] with using equation (1):

$$\rho_{\text{ex}} = \frac{m}{V} \quad (1)$$

where, " $\rho_{\text{ex}}$ " is the experimental density of specimen, " $m$ " is the weight of the specimen and " $V$ " is the volume of water displaced.

The microhardness was determined by an average of three readings for each sample using Vickers microhardnes machine as per ASTM E384-11 with a load of 500 g for 15 seconds. Thangarasu et al. [26] measured microhardnes using a microhardnes tester (MITUTOYO-MVK-H1) at 500 g load applied for 15 s. The dry sliding wear test was performed by the pin-on-disk machine as shown in Fig. 1 and it abides by stationary pin sliding on a rotating steel disk drive by an electric motor. The rotating counter disk was made of EN-32 steel which is with a hardness of HRC-65. The test samples were prepared as cylindrical with a diameter of 10 mm and length of 30 mm as shown in Fig. 2 from as-cast composite material and then the sample faces were metallographically polished. The wear tests were executed as per the ASTM G 99-95 standard at room temperature in dry sliding condition. The applied load was 20, 30 and 40 N, with sliding velocity at 1.5, 2.5 and 3.5 m/s and sliding distance of 2000 m were fixed for the wear test. The test pin mass was considered by a digital electronic balance with a least count of 0.0001 g before and after performed the wear test. The dry sliding wear rate of the fabricated composite can be measured by differentiating in the weight and which was converted into the volume loss using equation 2. The wear rates (W), SW and COF were calculated by equation 3, equation 4 and equation 5 [20,27].

$$\text{Volumeloss}(V) = \frac{m_1 - m_2}{\rho} \times 1000 \text{ mm}^3 \quad (2)$$

$$\text{Wear rate (W)} = \frac{V}{D} \text{ mm}^3/\text{m} \quad (3)$$

$$\text{Specific wear rate (SW)} = \frac{V}{D * L} \text{ mm}^3/\text{N} \cdot \text{m} \quad (4)$$

$$\text{Coefficient of friction } (\mu) = \frac{F_T}{F_N} \quad (5)$$

where  $m_1$  is the mass of the test pin before and  $m_2$  is the mass of test pin after the dry sliding wear test,  $\rho$  is the density of the test pin in  $\text{g}/\text{cm}^3$ ,  $D$  is the sliding distance in meter,  $F_T$  is the tangential forces and  $F_N$  is the normal force. The tangential force was measured from the load cell set in the pin-on-disk machine. The wear mechanism was studied with the worn surface morphology of aluminium composites by SEM analysis.



Fig. 1. Pin-on-Disc machine (top view).



Fig. 2. Dry sliding wear test pin of fabricated aluminium composite at various weight percent of BLA (a) 2 wt.%, (b) 4 wt.% and (c) 6 wt.%.

## 2.1 Taguchi method

Taguchi method was used for improvement of the quality of manufactured goods and also in

engineering applications, which is developed by Genichi Taguchi [28]. Taguchi method uses a standard design of orthogonal arrays to analyze the parameter effect with a finite number of trials for determined the optimal testing parameters [29]. The orthogonal array offers shortest feasible matrix in which effect of all parameters and their interactions is considered simultaneously. The testing parameters such as AL, SV, and BLA weight percentage (BL) and their levels are depicted in Table 3. The optimization of the testing parameter was determined with a typical  $L_{27}$  orthogonal array as shown in Table 4. The wear rate, SWR, and COF of the fabricated composites were considered as response variables. The statistical measurement of performance called signal-to-noise (S/N) ratio is determined and, it signify the quality characteristic, and biggest value of S/N ratio is essential for the optimal condition. Usually, that lower the better (LB), higher the better (HB) and nominal the better (NB) are the three performance characteristic used for the analysis of S/N ratio. In the case of minimization of wear rate, SWR, and COF, the S/N ratios with LB characteristic [30] need to be calculated by equation 6:

$$S/N = -10 \log \left( \frac{1}{n} \sum_{i=1}^n y_{ij}^2 \right) \quad (6)$$

where  $y_{ij}$  represent the  $i^{\text{th}}$  experiment at the  $j^{\text{th}}$  test, and  $n$  signify the total number of tests.

Table 3. Testing parameters and their levels.

Testing parameters	Unit	Level		
		1	2	3
AL	N	20	30	40
SV	m/s	1.5	2.5	3.5
BL	Wt. %	2	4	6

## 2.2 Grey relational analysis

GRA is relevant for solving problems with complex interrelationships between multiple parameters and variables [31], which was proposed by Deng [32]. The process of GRA is to as normalize wear rate, SWR, and COF obtained from experimental trials by using equation 7 between in the range of zero to one (0 to 1), and in next step the grey relational coefficient (GRC) is determined with the normalized data by equation 8. Then, the grey relational grade (GRG) by equation 9 is described by averaging



the GRC related to each process response. The general valuation of the multiple process responses is dependent on the GRG. The multiple process responses optimization can be renewed into optimization of a single GRG [29]. Optimization of a wear, SWR and COF parameters is the level of the largest GRG. In this process, a linear data preprocessing technique [20] for the wear rate, SWR and COF is the lower the better and indicated as equation 7.

$$X_i^*(k) = \frac{\max X_i(k) - X_i(k)}{\max X_i(k) - \min X_i(k)} \quad (7)$$

Where  $i = 1 \dots m$ ;  $k = 1 \dots n$ ;  $m$  is the number of experimental trials and  $n$  is the number of parameters, and  $X_i^*(K)$  is signify the normalized sequence,  $X_i(K)$  is signify the original sequence. After data preprocessing that the GRC ( $\xi_i(k)$ ) for the  $k^{\text{th}}$  performance characteristics in the  $i^{\text{th}}$  experiment is calculated by equation 8.

$$\xi_i(k) = \frac{\Delta_{\min} + \zeta \Delta_{\max}}{\Delta_{0i}(k) + \zeta \Delta_{\max}} \quad (8)$$

Where:

$$\Delta_{0i} = |X_0^*(K) - X_i^*(K)|, \Delta_{\min} = \min |X_0^*(K) - X_i^*(K)|$$

$$\Delta_{\max} = \max |X_0^*(K) - X_i^*(K)|$$

$X_0^*(K)$  signifies reference sequence and,  $X_i^*(K)$  signifies the comparison sequence and  $\zeta$  is the distinguishing coefficient, which ranges from 0 to 1 and normally  $\zeta$  is taken as 0.5. GRG ( $\gamma_i$ ) is the average value of the GRC and it is determined by equation 9:

$$\gamma_i = \frac{1}{n} \sum_{k=1}^n \xi_i(k) \quad (9)$$

The GRG plays important position to valuating the multiple performance characteristics and it deals the correlation between the reference sequence and the comparison sequence, with the highest GRG [33].

### 3. RESULTS AND DISCUSSION

#### 3.1 Microstructures analysis

The micrographs of the Al-4.5 wt.% Cu alloy, and at 2, 4 and 6 wt.% of BLA aluminium composites as shown in Fig. 3.

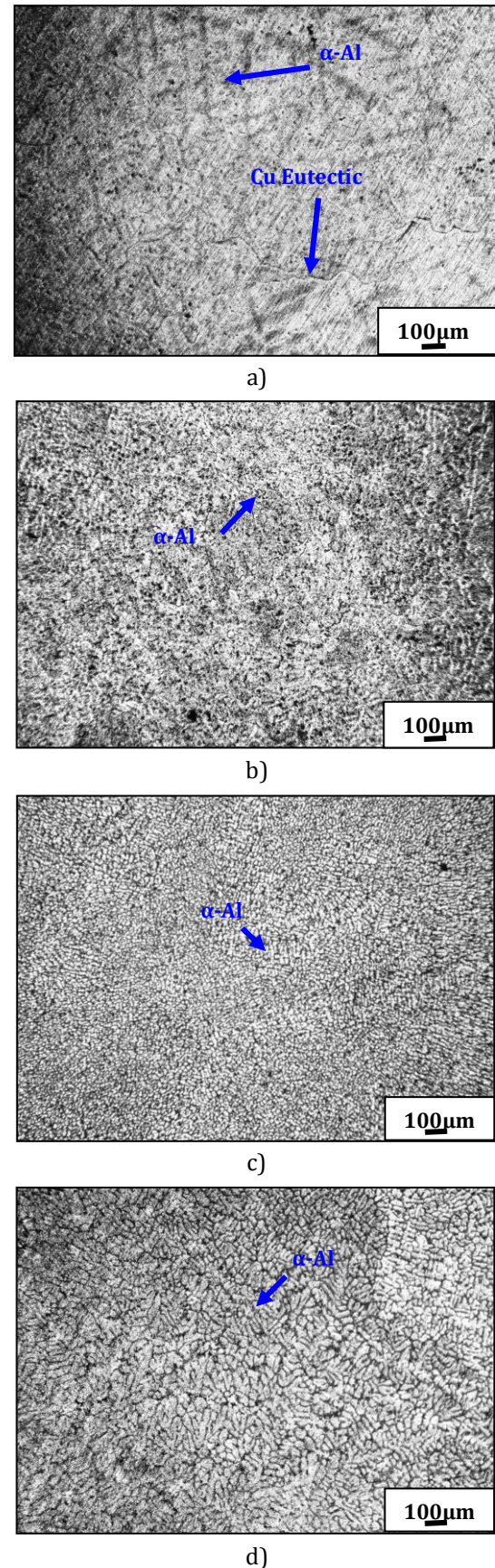


**Fig. 3.** Optical micrograph of (a) Al-4.5Cu alloy, (b) Al-4.5Cu-2BLA, (c) Al-4.5Cu-4BLA and (d) Al-4.5Cu-6BLA at weight percent composites with magnification of 100X.

The microstructure reveals the dendritic structure as shown in Fig. 3a which is due to supercooling during the period of solidification. The cooling rate is very high and is known as supercooling, which forms the dendritic structure. The dendritic structure is characterized with elongated primary  $\alpha$  (Al) dendritic arms which have high aspect ratios.

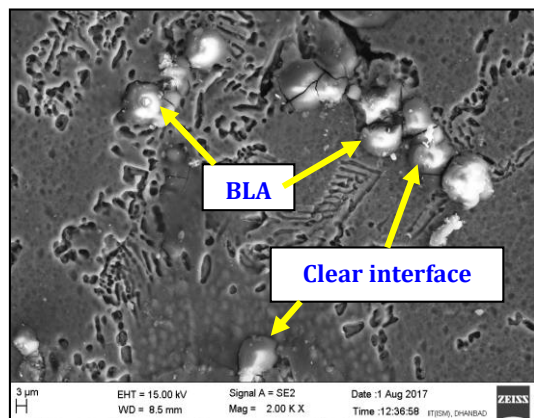


**Fig. 4.** SEM micrograph of Al-4.5Cu-6BLA composite at magnification of 2.00 K X.

The dendritic structure of the matrix alloy was refined and form grain structure with the addition of BLA as shown in Figs. 3b-3d. The grain refinement may take place due to BLA particles which act as grain nucleation sites and aluminium grains solidifies on grain refiner. The constitution under cooling zone in front of the BLA particles may cause it to act as a grain nucleation site. Formation of interfacial nucleation sites is increased in composite with an increased weight fraction of BLA particles. The spreading of BLA particles in the aluminium matrix restricts the growth of  $\alpha$  (Al) grains during solidification. The higher the content of BLA particles, the more the grain nucleation sites are created as well as the more the resistance is offered to the freely growing  $\alpha$  (Al) grains, therefore, the grains are further refined [34]. The grain refinement promotes to achieve the improvement of mechanical and tribological properties of the fabricated composite materials [35]. The uniformly incorporation of BLA particles and the clear interface was observed between the matrix alloy and BLA particles as shown in Fig. 4.

### 3.2 Density and Hardness

The density was influenced with the addition of BLA particles in the fabricated aluminium

composites as shown in Fig. 5. It was observed that as BLA content increased, the density of the fabricated composites was decreased. The composite consisting of 2, 4 and 6 wt.% of BLA particles, it was observed that the reductions in density at 1.677 %, 3.25 % and 4.895 % in comparison with Al-4.5 wt.% Cu alloy as shown in Fig. 5. The maximum reduction in density that is 2.619 g/cm<sup>3</sup> was observed in the Al-4.5Cu/6BLA composite in comparison with matrix alloy is 2.7538 g/cm<sup>3</sup>. The reason may be the BLA particles expressed lower density than matrix alloy. Similar results were noticed in the earlier research that the density of the aluminium composites was decreased with addition of fly ash content [36] and also reported same with the addition of RHA in the aluminium composites [37].

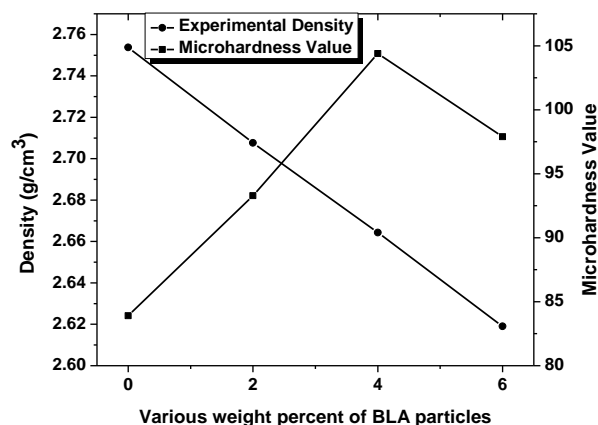


**Fig. 5.** Density and Microhardness of the fabricated aluminium composites.

The microhardness of the Al-4.5 wt.% Cu alloy with 2, 4 and 6 wt.% addition of BLA particles as shown in Figure 6. It was noticed that the hardness of the fabricated aluminium composites increased significantly with addition of BLA particles. It was observed that microhardness values increased by 11.19 %, 24.43 % and 16.68 % for composites which containing 2, 4 and 6 wt. % of BLA content in composites respectively in comparison with Al-4.5wt.% Cu alloy as shown in Figure 5. The highest value of hardness is 104.4 observed in the Al-4.5Cu/6BLA composite in comparison with matrix alloy. An increase in the hardness of composites indicates that the presence the BLA particles in the matrix have improved the overall hardness of the composites due to the matrix is soft material and, the reinforcement particles being hard and enhance the overall hardness of the composites. The hardness

increased or decreased linearly of the composite due to the addition of ceramic phase in the matrix alloy with the presence of reinforcement particles [38].

### 3.3 Effect of parameters on dry sliding wear behavior

The dry sliding wear results of the fabricated aluminium composites and process variables considered such as wear rate, SWR, and COF were depicted in Table 4 as per standard  $L_{27}$  orthogonal array. The applied load, sliding velocity, and the weight percent of BLA as control parameters influence on the wear rate, SWR and COF was analyzed with S/N ratios with using equation (6) of the composite as depicted in Table 4. The higher S/N ratio value is corresponds to the better execution.

The GRC and GRG values for each corresponding experimental trial are determined by equation (8) and equation (9) as depicted in Table 5. The ranking was

assigned to corresponding GRG as depicted in Table 5 in order of importance of the testing parameters over the dry sliding wear behavior. The larger value of the GRG signifies that the corresponding dry sliding wear parameters are consider as optimal condition. The average GRG for each level and total average GRG of dry sliding wear parameters was calculated as per Taguchi method as shown in Table 6. And also the average GRG values as shown in Figure 6 and where the dashed line indicates that the total average of the GRG. The sign (\*) used to signify the optimum value of GRG as depicted in Table 6. Based on the GRG results depicted in Table 6 and Figure 6, the optimal condition for the combined wear rate, SWR and COF is at 20N AL (level 1), 4 m/s SV (level 3), and at 4 wt.% of BLA (level 2) combination is attained. The rank assigned for corresponding GRG which signify the strongest parameter in the dry sliding wear performance as shown in Table 5. This results revealed that AL is strongly effected the dry sliding wear behavior.

**Table 4.** Dry sliding wear results of fabricated aluminium composites.

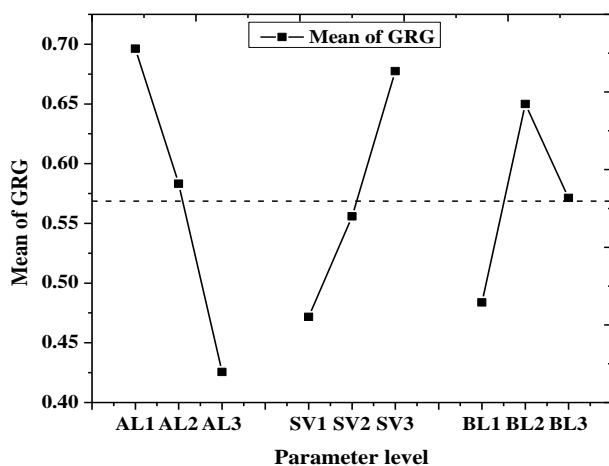
Exp. No.	Testing parameters			Dry sliding wear results			S/N ratios		
	AL (N)	SV (m/s)	BL (%)	Wear rate ( $\text{mm}^3/\text{m}$ )	SWR ( $\text{mm}^3/\text{N-m}$ )	COF	Wear rate	SWR	COF
1	20	1.5	2	0.0029051	0.00014525	0.514	50.7367	76.7573	5.7807
2	20	1.5	4	0.0023881	0.00011941	0.378	52.4389	78.4595	8.4502
3	20	1.5	6	0.0024421	0.00012211	0.383	52.2447	78.2653	8.3360
4	20	2.5	2	0.0022601	0.00011301	0.406	52.9174	78.9381	7.8295
5	20	2.5	4	0.0017882	0.00008941	0.323	54.9516	80.9722	9.8159
6	20	2.5	6	0.0018209	0.00009104	0.345	54.7942	80.8148	9.2436
7	20	3.5	2	0.0019571	0.00009785	0.356	54.1677	80.1883	8.971
8	20	3.5	4	0.0012971	0.00006485	0.306	57.7405	83.7611	10.286
9	20	3.5	6	0.0015824	0.00007912	0.312	56.0136	82.0342	10.117
10	30	1.5	2	0.0038012	0.00012671	0.578	48.4015	77.9440	4.7614
11	30	1.5	4	0.0025293	0.00008431	0.529	51.9399	81.4824	5.5309
12	30	1.5	6	0.0034086	0.00011362	0.546	49.3484	78.8909	5.2562
13	30	2.5	2	0.0036014	0.00012004	0.557	48.8705	78.413	5.0829
14	30	2.5	4	0.0020928	0.00006976	0.436	53.5854	83.1278	7.2103
15	30	2.5	6	0.0032366	0.00010788	0.464	49.7982	79.3406	6.6696
16	30	3.5	2	0.0025589	0.00008529	0.538	51.8389	81.3813	5.3844
17	30	3.5	4	0.0015874	0.00005291	0.429	55.9862	85.5287	7.3509
18	30	3.5	6	0.0019916	0.00006638	0.411	54.0159	83.5583	7.7232
19	40	1.5	2	0.0062108	0.00015527	0.643	44.1371	76.1782	3.8358
20	40	1.5	4	0.0050805	0.00012701	0.536	45.8818	77.9231	5.4167
21	40	1.5	6	0.0056707	0.00014176	0.628	44.9272	76.9684	4.0408
22	40	2.5	2	0.0055252	0.00013813	0.632	45.1530	77.1942	3.9857
23	40	2.5	4	0.0043602	0.00010901	0.496	47.2098	79.2511	6.0904
24	40	2.5	6	0.0048273	0.00012068	0.593	46.3259	78.3671	4.5389
25	40	3.5	2	0.0039884	0.00009971	0.629	47.9840	80.0252	4.0269
26	40	3.5	4	0.0032579	0.0000814	0.471	49.7412	81.7824	6.5396
27	40	3.5	6	0.0037583	0.00009395	0.547	48.5001	80.5413	5.2403

**Table 5.** The calculated GRC and GRG.

Exp. No.	Normalized			GRC			GRG	Rank
	Wear rate	SWR	COF	Wear rate	SWR	COF		
1	0.67275	0.09785	0.38279	0.604413	0.356596	0.4475431	0.46951764	17
2	0.77796	0.35040	0.78635	0.692489	0.434936	0.7006237	0.60934926	9
3	0.76698	0.32403	0.77151	0.682107	0.425179	0.6863544	0.59788016	11
4	0.80402	0.41293	0.70326	0.718407	0.459953	0.6275605	0.60197334	10
5	0.90005	0.64345	0.94955	0.833406	0.583737	0.9083558	0.77516626	4
6	0.89339	0.62748	0.88427	0.824263	0.573051	0.8120482	0.73645384	5
7	0.86568	0.56094	0.85163	0.788245	0.53245	0.7711671	0.69728716	7
8	1	0.88335	1	1	0.810831	1	0.93694350	1
9	0.94193	0.74398	0.98219	0.895952	0.66136	0.9656161	0.84097598	2
10	0.49038	0.27907	0.19288	0.495239	0.409523	0.3825198	0.42909403	22
11	0.74923	0.69327	0.33829	0.665984	0.619791	0.4303959	0.57205682	12
12	0.57028	0.40692	0.28783	0.537799	0.457424	0.4124847	0.46923592	18
13	0.53105	0.34414	0.25519	0.516021	0.432577	0.4016686	0.45008883	20
14	0.83806	0.83543	0.61424	0.755359	0.752363	0.5644891	0.69073702	8
15	0.6052	0.46294	0.53116	0.558839	0.482131	0.5160796	0.51901642	15
16	0.74321	0.68364	0.31157	0.660682	0.612473	0.4207241	0.56462637	14
17	0.94092	1	0.63501	0.894321	1	0.5780446	0.82413288	3
18	0.85866	0.86838	0.68843	0.779615	0.79162	0.6160877	0.72910788	6
19	0	0	0	0.333333	0.333336	0.3333333	0.33333406	27
20	0.23003	0.27608	0.31751	0.393712	0.408524	0.4228356	0.40835703	23
21	0.10992	0.13193	0.04451	0.359693	0.365478	0.3435270	0.35623236	26
22	0.13953	0.16746	0.03264	0.367521	0.375225	0.3407482	0.36116469	25
23	0.37662	0.45201	0.43620	0.445087	0.477104	0.4700139	0.46406832	19
24	0.28156	0.33792	0.14837	0.410362	0.430264	0.3699232	0.40351657	24
25	0.45228	0.54282	0.04154	0.477231	0.522368	0.3428281	0.44747579	21
26	0.60095	0.72124	0.51038	0.556145	0.642048	0.5052474	0.56781346	13
27	0.49912	0.59902	0.28486	0.499559	0.554953	0.4114774	0.48866291	16

**Table 6.** Response table for grey relational grade.

Sym	Level 1	Level 2	Level 3	Delta	Rank
AL	0.696172*	0.583122	0.425625	0.270547	1
SV	0.471673	0.555798	0.677447*	0.205774	2
BL	0.48384	0.649847*	0.571231	0.166007	3
Average grey relational grade: 0.568306242					

**Fig. 6.** Effect of testing parameters on grey relational grade.

### 3.4 Analysis of Variance

The influence of parameters and their interaction on a particular response were analyzed with ANOVA. The obtained results from ANOVA are used to describe that which independent parameter has more influence over the other, and also analyzed to get the percentage contribution of that particular independent parameter. From the Table 7 and Fig. 7, it was concluded that the test parameters such as the applied load (48 %), sliding velocity (28 %) and percentage of BLA (18 %) have great effect at the confidence level of 95 % on GRG of fabricated aluminium composites. The highest mean GRG values are 0.696172, 0.677447 and 0.649847 observed at level 1 of applied load contribution, at level 3 of sliding velocity contribution and at level 2 of percentage of BLA contribution respectively. The interactions of parameters are effected at minimum percentage resulting they may be statistically insignificant.

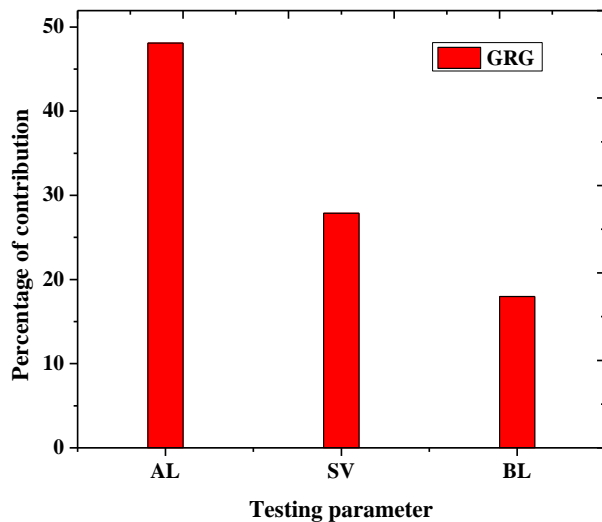


**Table 7.** ANOVA results of GRG.

Parameters	Sum of squares	Degree of freedom	Mean sum of squares	F-test	Percentage of contribution
L	0.33234354	2	0.16617177	325.794298	48.09888
V	0.1926558	2	0.0963279	188.859281	27.88238
B	0.12412791	2	0.06206395	121.681816	17.96458
L×V	0.0164285	4	0.00410713	8.05238042	2.377638
V×B	0.0152256	4	0.0038064	7.46277886	2.203545
L×B	0.00609729	4	0.00152432	2.98856688	0.882438
Errors	0.00408041	8	0.00051005	...	0.590543
Total	0.69095904	26	0.02657535	...	100

**Table 8.** Results of confirmation test for GRG as combined wear rate, SWR and COF.

	Initial	Optimal	
		Predicted value	Experimental value
Level	L1 V1 B1	L1 V3 B2	L1 V3 B2
Wear rate	0.0029051	...	0.0012971
Specific wear rate	0.000145255	...	0.000064855
COF	0.514	...	0.306
Grey relational grade	0.469517646	0.886854	0.936943503
Improvement of GRG = 0.4674258			

**Fig. 7.** Grey relational grade of the contribution percentage of each parameter.

### 3.5 Confirmation experiments

The optimum condition of the dry sliding wear parameters was described and the confirmation test was performed to check the validity of the analysis. In the confirmatory test, the optimum combination was set, and the trial test was performed. The predicted value ( $\hat{\gamma}$ ) using optimum level of dry sliding wear parameters is calculated with equation 10 [29].

$$\hat{\gamma} = \gamma_m + \sum_{i=1}^q (\bar{\gamma}_i - \gamma_m) \quad (10)$$

Where  $\gamma_m$  is the total mean of GRG,  $\bar{\gamma}_i$  is the GRG mean at the optimum level, and  $q$  is the number

of main design parameters that appreciably affect the wear rate, SWR, and COF.

The predicted and the experimental values of GRG were depicted in Table 8 at optimal parameters. The comparison of the predicted GRG with the calculated GRG obtained by confirmation experiments using the optimal testing parameters and also compared with initial testing parameters. The GRG was improved significantly and therefore, present approach for optimization of testing parameters for multiple responses is feasible.

### 3.6 Wear rate of BLA reinforced composites compared with matrix alloy

The variation in wear rate of the matrix alloy and BLA reinforced composites as shown in Fig. 8. It is described that the wear rate of the composite decreased with the addition of BLA particulates. The wear rate 16.11 % decreased with the addition of 2 wt.% of BLA, and 31.04 % at 4 wt.% of BLA and 29.48 % at 6 wt.% of BLA in the composites when compared with matrix alloy at applied load of 20 N and sliding velocity 1.5 m/s as shown Fig. 8. The wear rate of Al-4.5Cu/BLA composites is lower than that of the matrix alloy, which indicates the wear resistance of the composites increased with addition BLA. The hardness of the fabricated composites is also key point to enhance the wear resistance. The incorporation of BLA particles remarkably strengthened the hardness of the fabricated

composites that leads to reduce the wear rate as shown in Fig. 8.

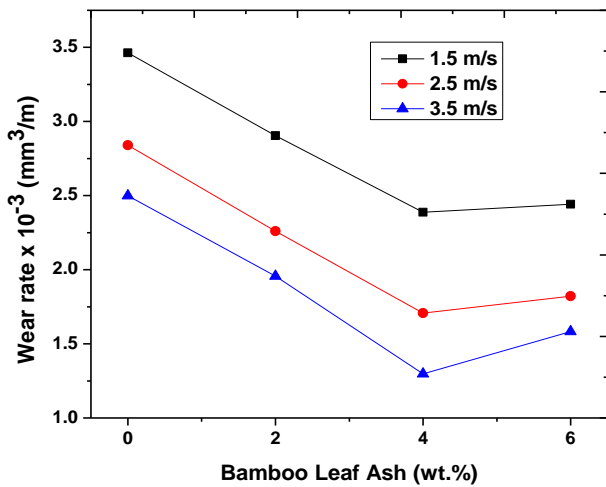


**Fig. 8.** Effect of weight percent of BLA on wear rate of composites at 20 N.

The reduction in wear of the composites may be owed to combination of metallurgical bonding between the BLA particles and matrix, and hardness. The contact area between the matrix and BLA particles increased as increased the BLA content resulting bonding strength of composites increased. BLA particles act as a load bearing elements during dry sliding wear test.

### 3.7 Parameters effect on dry sliding wear behavior with Morphology of worn surfaces

The dry sliding wear mechanism was observed with the SEM images of worn out samples of at 0, 2, 4 and 6 wt.% of BLA composites as shown in Fig. 9 with effect of a parameter such as AL, SV and BL. It was noticed that the wear rate, SWR, and COF of matrix alloy is much higher than the BLA reinforced composite irrespective of AL and SV.

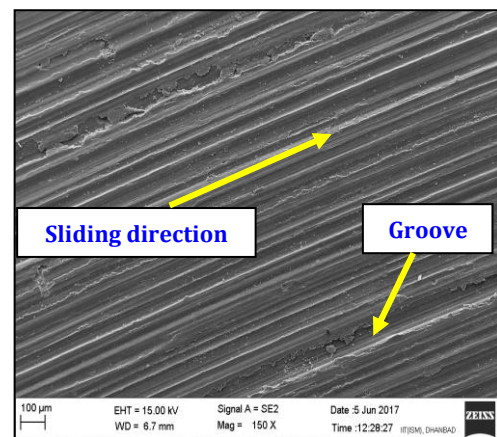
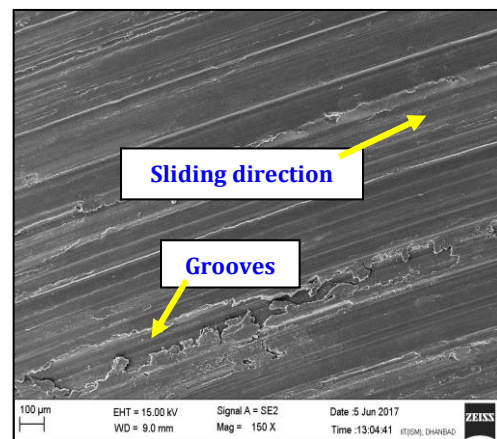
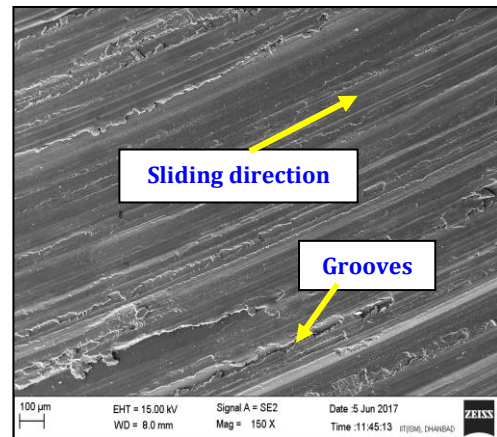
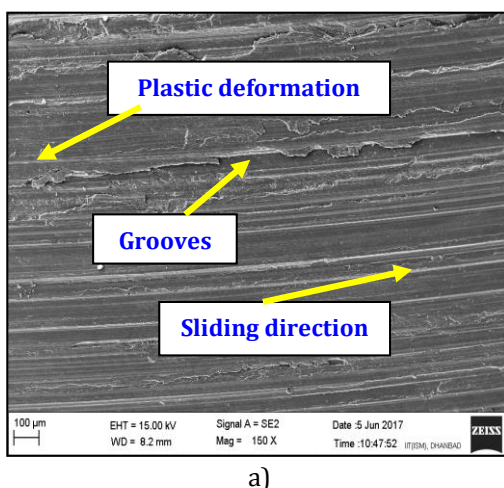


**Fig. 9.** SEM micrograph of worn surface of (a) Al-4.5Cu alloy, (b) Al-4.5Cu-2BLA, (c) Al-4.5Cu-4BLA and (d) Al-4.5Cu-6BLA at weight percent composites at AL = 20N and SV = 1.5 m/s at magnification of 150x.

From the worn out morphology of Al-4.5Cu alloy as shown in Fig. 9a it is observed that material removal rate was higher and shown deep and plowing grooves.

The plastic deformation at the edges of the groove is larger and it initiates the subsurface cracking, which might lead to severe removal of

material and Ferit and Sakip [39] also reported similar results. The matrix alloy was undergoes heavy plastic deformation on the surface which leads to the high wear rate due to the matrix was softer than the BLA reinforced composites. The hardness of the fabricated composites was shown in Fig. 5. The hardness increased with addition of BLA particles and these results are very effective to reduce the wear rate, SWR and COF remarkably. It was observed that the addition of BLA particles wear rate, SWR and COF of composites was significantly reduced in comparison to the matrix alloy. As the BLA content increase in the matrix, the deepness and number of grooves on the worn surface were decreased as shown in Figs. 9b-9d. Comparatively, minor plastic deformation observed at the edge of the grooves, and smaller grooves were observed in the path of sliding direction in the fabricated composites. It may be because the BLA particles tend to protect the matrix alloy from direct contact with the counterpart, resulting in increased the resistance to wear by reinforcement particles. Baradeswaran and Perumal [40] also observed that the wear rate was decreased significantly with the addition of  $B_4C$  particles in the aluminium composite.

The effect of applied load on dry sliding behavior was observed from the micrograph of worn out surfaces as shown in Fig. 9b and Fig. 10a at lower load to higher load. The increase in applied load that leads to increase in the wear rate, SWR, and COF as depicted in Table 4. This may be due to the higher level of plastic deformation, which further leads to a chance of sub surface cracking and delamination [19] as shown in Fig. 10a.

The dry sliding wear was influenced with the microstructural properties of the composites, and also on the type of loading contact situation. According to Archard's statement [41] that the amount of dry sliding wear is typically proportional to the applied load and the sliding distance and is inversely proportional to the hardness of the surface is worn out. These results are in good agreement with Kok and Ozdin [42] who suggested that the severe wear rate in the matrix alloy and composite was observed by increase in applied load and Ashok et al. [43] also observed that the delaminated area on worn out surface and plastic

deformation at the edges of grooves of the aluminium composite addition with ALN particles at higher applied load. At lower load, the mild wear rate with lower COF and SWR observed in the fabricated composites at lower load due to BLA particles were act as load-bearing elements as they remain intact without fissure. As the load increase the deeper grooves was observed and also the induced stresses may transcend the fracture strength of the BLA particles which may result in fracture. The fracture hard BLA particles scrape the soft matrix alloy that leads to severe the wear rate and at higher load the plastic flow of the material may be dominant.

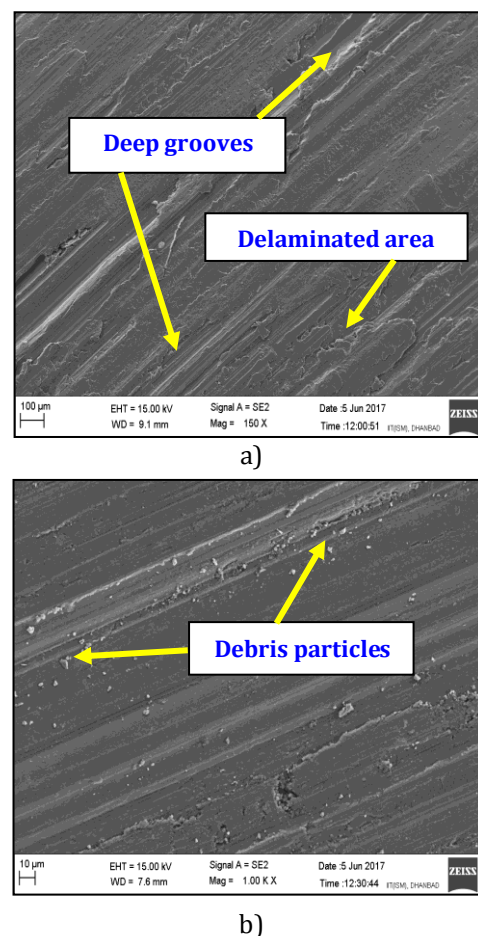


**Fig. 10.** SEM micrograph of worn surface of (a) Al-4.5Cu-2BLA at AL = 40N and SV = 1.5 m/s and at magnification of 150x (b) Al-4.5Cu-6BLA at AL=20 N and SV=3.5 m/s composites at magnification of 1.00Kx.

The effect of sliding velocity as shown in Fig. 9d and Fig. 10b, it was observed that the wear rate, SWR, and COF minimized with increase in sliding velocity as depicted in Table 4. When sliding velocity was increased, the travel time was decreased to complete the required sliding distance (2000 m), this may cause the



generation of wear debris particles which significantly decreased and might be resulting in a reduction of wear rate of the composite as shown in Fig. 10b. Ravikiran and Surappa [44] also observed that as sliding velocity increased the wear rate and COF decreased of the Al-30%SiC MMC. At increase in sliding velocity, the wear rate was increased initially due to direct contact between the hard reinforcement particles and rotating disc. Further increase of velocity the wear rate was decreased. As the sliding velocity increased the interfacial temperature was increased which may accelerate the oxidation of matrix alloy resulting in the formation of a thick oxide layer [45]. The oxide layer acts as a protective shroud by inhibiting the metal to metal direct contact among the pin surface and counter disc surface and decrease the wear rate and COF.

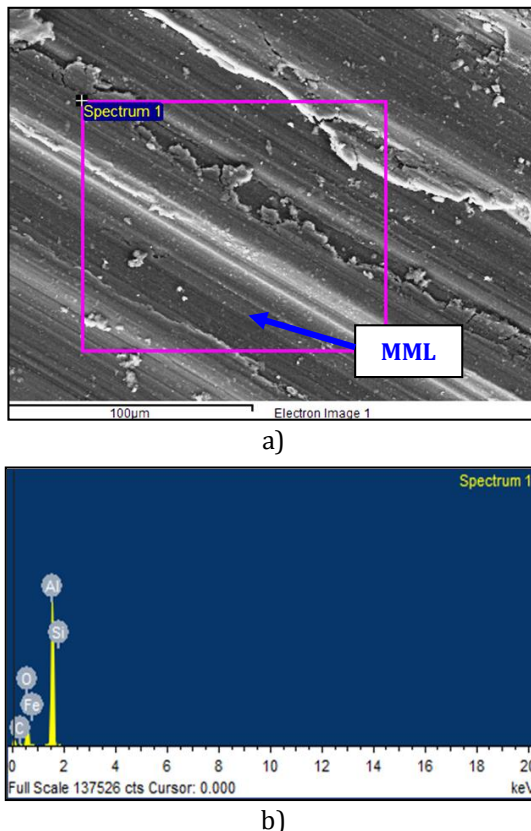


**Fig. 11.** SEM micrograph of worn surface (a) with EDAX profile (b) at AL = 20N and SV = 3.5 m/s of Al-4.5Cu-6BLA at weight percent composites.

Mavros et al. [46] has observed the forming of the oxide layer in the case of AlMgSi-TiC composite reduced the wear rate. It was noted that the iron particles were oxidized from the counter face during sliding. The embodiment of a stable and thick mechanical mixed layer

consist of aluminium and iron oxides and also fractured BLA particles acted as an insulation layer among the pin surface and counter steel disc thus decreased the wear rate COF. The presence of oxygen and iron was noted in the Energy Dispersive Analysis of X-ray (EDAX) profile of the worn surfaces as shown in Fig. 11. The presence of iron approved that transfer of iron particles from the counter body of steel disk to the worn surface of the composite pin, as oxygen also indicated the oxidation reaction.

From these results, it maybe concluded that the shifting and mechanical mixing of materials have been taken into between two sliding surfaces, result in to the formation of an MML on the worn surfaces. Similar, results also observed by earlier researchers [47,48]. The MML is confirmed with the SEM micrograph of fabricated aluminium composite as shown in Fig. 11.

#### 4. CONCLUSION

The BLA was extruded from agro waste and used as reinforcement to fabricated economical AMMCs by stir casting method. The microstructural modification was observed in the matrix alloy with the addition of BLA. The grain refinement noticed in the composites micrograph due to BLA particles may acts as grain refiner and clear interface was observed between matrix and reinforcement particles by optical and SEM images. The density of the composites was decreased with the addition of BLA content and conversely, the hardness of the composite was increased in comparison with matrix alloy. The standard  $L_{27}$  orthogonal array of Taguchi method coupled with GRA is used to optimize the multiple performances of dry sliding wear behavior of the aluminium composite reinforced with BLA. For the combined optimal level for wear rate, SWR and COF is observed with GRG that at 20 N applied load, 3.5 m/s sliding velocity and 4 wt.% of BLA. Based on the ANOVA results, the applied load (48 %) is the most influenced on GRG (combined wear rate, SWR, and COF) and followed by sliding velocity is 28 % and the weight percentage of BLA is 18 %. The interaction between applied load, sliding velocity and the weight percent of BLA influenced on the dry sliding wear is a statistically insignificant. The optimum combination of test parameters selected



based on highest GRG and compared with predicted value and also confirmed with the experimental trials. Wear mechanism was analyzed with worn out surfaces by SEM revealed that the mild wear rate and lower COF were observed at lower load due to BLA particles act as load bearing elements. At higher load the deeper grooves and plastic deformation at grooves edges were observed resulting in severe wear rate. And the lower wear rate was found at higher velocity and lower load, whereas higher wear rate was observed at higher velocity and higher load. It was noticed that the MML is formed and decreased the wear rate at higher velocity.

## Acknowledgement

Authors would like to acknowledge the National Institute of Technology Manipur (NITM), Imphal, India-795004 for financial support to carry out the Experimental research work of Mr. B. Praveen Kumar, Full Time Research Scholar, Enrolment Number (15PME004), under the guidance of Dr. Anil Kumar Birru, Assistant Professor and Head, Department of Mechanical Engineering, NITM.

## REFERENCES

- [1] A. Vencel, A. Rac, I. Bobic, *Tribological Behaviour of Al-Based Mmcs and Their Application in Automotive Industry*, *Tribology in Industry*, vol. 26, no. 3-4, pp. 31-38, 2004.
- [2] M. Koji, H. Makoto, F. Ryosuke, K. Teruto, *Effects of Alloying Elements in Aluminum Alloys and Activations on Zincate Treatment and Electroless Nickel-Phosphorus Plating*, *Materials Transactions*, vol. 51, iss. 1, pp. 78-84, 2010, doi: [10.2320/matertrans.L-M2009830](https://doi.org/10.2320/matertrans.L-M2009830)
- [3] D.I. Adeyemi, A. Bolaji, O.A. Mosobalaje, J.O. Oluyemi, D.S. Moshood, *Effect of Heat Treatment on Some Mechanical Properties of 7075 Aluminium Alloy*, *Materials Research*, vol. 16, no. 1, pp. 190-194, 2013, doi: [10.1590/S1516-14392012005000167](https://doi.org/10.1590/S1516-14392012005000167)
- [4] J.S. Benjamin, M.J. Bomford, *Dispersion strengthened aluminum made by mechanical alloying*, *Metallurgical Transactions A*, vol. 8, iss. 8, pp. 1301-1305, 1977, doi: [10.1007/BF02643845](https://doi.org/10.1007/BF02643845)
- [5] G.J. Allwyn Kingsly, S.N. Mohamed, I. Dinaharan, R.S.J. David, *Production and characterization of rich husk ash particulate reinforced AA6061 aluminum alloy composites by compocasting*, *Transaction of Nonferrous Metal Society of China*, vol. 25, iss. 3, pp. 683-691, 2015, doi: [10.1016/S1003-6326\(15\)63653-6](https://doi.org/10.1016/S1003-6326(15)63653-6)
- [6] D. Milosavljevic, G. Jovicic, *Properties of Metal Matrix Composites for Automotive Applications*, *Tribology in Industry*, vol. 24, no. 3-4, pp. 43-46, 2002.
- [7] J. Lakshmipathy, B. Kulendran, *Reciprocating Wear Behaviour of 7075Al/SiC and 6061Al/Al<sub>2</sub>O<sub>3</sub> Composites: A study of Effect of Reinforcement, Stroke and Load*, *Tribology in Industry*, vol. 36, no. 2, pp. 117-126, 2014.
- [8] M.R. Rahimipour, A.A. Tofigh, M.O. Shabani, P. Davami, *The Enhancement of Wear Properties of Compo-Cast A356 Composites Reinforced with Al<sub>2</sub>O<sub>3</sub> Nano Particulates*, *Tribology in Industry*, vol. 36, no. 2, pp. 220-227, 2014.
- [9] A. Amin, S. Ali, N. Omid, F. Hamid, S. Saeid, *Optimizing consolidation behavior of Al 7068-TiC nanocomposites using Taguchi statistical analysis*, *Transaction of Nonferrous Metal Society of China*, vol. 25, iss. 8, pp. 2499-2508, 2015, doi: [10.1016/S1003-6326\(15\)63868-7](https://doi.org/10.1016/S1003-6326(15)63868-7)
- [10] S. Poria, G. Sutradhar, P. Sahoo, *Wear and Friction Behavior of Stir Cast Al-TiB<sub>2</sub> Metal Matrix Composites with Various Lubricants*, *Tribology in Industry*, vol. 38, no. 4, pp. 508-521, 2016.
- [11] N. Selvakumar, B. Gnanasundarajayaraja, P. Rajeshkumar, *Enhancing the Properties of Al-WC Nanocomposites Using Liquid Metallurgy*, *Experimental Techniques*, vol. 40, iss. 1, pp. 129-135, 2016, doi: [10.1007/s40799-016-0015-y](https://doi.org/10.1007/s40799-016-0015-y)
- [12] J.J. Moses, S.J. Sekhar, *Dry Sliding wear behavior of silicon carbide particulate reinforced AA6061 aluminum alloy composites produced via stir casting*, *Advanced Materials Research*, vol. 984-985, pp. 221-226, 2014, doi: [10.4028/www.scientific.net/AMR.984-985.221](https://doi.org/10.4028/www.scientific.net/AMR.984-985.221)
- [13] S. Suresh, N.S.V. Moorthi, S.C. Vettivel, N. Selvakumar, *Mechanical behavior and wear prediction of stir cast Al-TiB<sub>2</sub> composites using response surface methodology*, *Materials and Design*, vol. 59, pp. 383-396, 2014, doi: [10.1016/j.matdes.2014.02.053](https://doi.org/10.1016/j.matdes.2014.02.053)
- [14] A. Bahrami, N. Soltani, M.I. Pech-Canul, C.A. Gutiérrez, *Development of metal-matrix composites from industrial/agricultural waste materials and their derivatives*, *Critical Reviews in Environmental Science and Technology*, vol. 46, iss. 2, pp. 143-208, 2016, doi: [10.1080/10643389.2015.1077067](https://doi.org/10.1080/10643389.2015.1077067)
- [15] N. Soltani, A. Bahrami, M.I. Pech-Canul, L.A. González, *Review on the physicochemical*

- treatments of rice husk for production of advanced materials, Chemical Engineering Journal, vol. 264, pp. 899-935, 2015, doi: [10.1016/j.cej.2014.11.056](https://doi.org/10.1016/j.cej.2014.11.056)
- [16] A. Apasi, P.B. Madakson, D.S. Yawas, V.S. Aigbodon, *Wear Behaviour of Al-Si-Fe Alloy/Coconut Shell Ash Particulate Composites*, Tribology in Industry, vol. 34, no. 1, pp. 36-43, 2012.
- [17] S.D. Saravanan, M. Senthilkumar, S. Shankar, *Effect of Particle Size on Tribological Behavior of Rice Husk Ash-Reinforced Aluminum Alloy (AlSi10Mg) Matrix Composites*, Tribology Transactions, vol. 56, iss. 6, pp. 1156-1167, 2013, doi: [10.1080/10402004.2013.831962](https://doi.org/10.1080/10402004.2013.831962)
- [18] J.B. Rao, D.V. Rao, K.S. Prasad, N. Bhargava, *Dry sliding wear behaviour of fly ash particles reinforced AA 2024 composites*, Materials Science-Poland, vol. 30, iss. 3, pp. 204-211, 2012, doi: [10.2478/s13536-012-0026-z](https://doi.org/10.2478/s13536-012-0026-z)
- [19] M. Senthilkumar, S.D. Saravanan, S. Shankar, *Dry sliding wear and friction behavior of aluminum-rice husk ash composite using Taguchi's technique*, Journal of composite materials, vol. 49, iss. 18, pp. 2241-2250, 2015, doi: [10.1177/0021998314545185](https://doi.org/10.1177/0021998314545185)
- [20] S. Dharmalingam, R. Subramanian, V.K. Somasundara, B. Anandavel, *Optimization of Tribological Properties in Aluminum Hybrid Metal Matrix Composites Using Gray-Taguchi Method*, Journal of Materials Engineering and Performance, vol. 20, iss. 8, pp. 1457-1466, 2011, doi: [10.1007/s11665-010-9800-4](https://doi.org/10.1007/s11665-010-9800-4)
- [21] S. Rajesh, K.S. Thirumalai, M. Uthayakumar, M. Pethuraj, *Process Optimization and Wear Behavior of Red Mud Reinforced Aluminum Composites*, Advances in Tribology, vol. 2016, pp. 1-7, 2016, doi: [10.1155/2016/9082593](https://doi.org/10.1155/2016/9082593)
- [22] S. Rajesh, A.G. Krishna, P.R.M. Raju, D. Muthukannan, *Application of grey-taguchi method for optimization of dry sliding wear properties of aluminum MMCs*, Frontiers of Mechanical Engineering, vol. 7, iss. 3, pp. 279-287, 2012, doi: [10.1007/s11465-012-0329-0](https://doi.org/10.1007/s11465-012-0329-0)
- [23] B.P. Kumar, B.A. Kumar, *Microstructure and mechanical properties of aluminium metal matrix composites with addition of bamboo leaf ash by stir casting method*, Transaction of Nonferrous Metal Society of China, vol. 27, iss. 12, pp. 2555-2572, 2018, doi: [10.1016/S1003-6326\(17\)60284-X](https://doi.org/10.1016/S1003-6326(17)60284-X)
- [24] P. Suswagata, S. Prasanta, S. Goutam, *Tribological Characterization of Stir-cast Aluminium-TiB<sub>2</sub> Metal Matrix Composites*, Silicon, vol. 8, iss. 4, pp. 591-599, 2016, doi: [10.1007/s12633-016-9437-5](https://doi.org/10.1007/s12633-016-9437-5)
- [25] A. Mazahery, M.O. Shabani, *Characterization of cast A356 alloy reinforced with nano SiC composites*, Transaction of Nonferrous Metal Society of China, vol. 22, iss. 2, pp. 275-280, 2012, doi: [10.1016/S1003-6326\(11\)61171-0](https://doi.org/10.1016/S1003-6326(11)61171-0)
- [26] A. Thangarasu, N. Murugan, I. Dinaharan, S.J. Vijay, *Microstructure and microhardness of AA1050/TiC surface composite fabricated using friction stir processing*, Sadhana, vol. 37, iss. 5, pp. 579-586, 2012, doi: [10.1007/s12046-012-0097-x](https://doi.org/10.1007/s12046-012-0097-x)
- [27] N. Radhika, R. Raghu, *Evaluation of Dry Sliding Wear Characteristics of LM 13 Al/B4C Composites*, Tribology in Industry, vol. 37, no. 1, pp. 20-28, 2015.
- [28] J.L. Rosaa, A. Robina, M.B. Silvab, C.A. Baldan, M.P. Peres, *Electrodeposition of copper on titanium wires: Taguchi experimental design approach*, Journal of materials processing technology, vol. 209, iss. 3, pp. 1181-1188, 2009, doi: [10.1016/j.jmatprotec.2008.03.021](https://doi.org/10.1016/j.jmatprotec.2008.03.021)
- [29] C.L. Lin, *Use of the Taguchi Method and Grey Relational Analysis to Optimize Turning Operations with Multiple Performance Characteristics*, Materials and Manufacturing Processes, vol. 19, iss. 2, pp. 209-220, 2004, doi: [10.1081/AMP-120029852](https://doi.org/10.1081/AMP-120029852)
- [30] A. Amit, S. Amit, P. Amar, *Study on mechanical and wear characterization of novel Co30Cr4Mo biomedical alloy with added nickel under dry and wet sliding conditions using Taguchi approach*, Proceedings of the Institution of Mechanical Engineers, Part L: Journal of Materials Design and Applications, 2015, doi: [10.1177/1464420716638112](https://doi.org/10.1177/1464420716638112)
- [31] Y. Kuo, T. Yang, G.-W. Huang, *The use of a grey-based Taguchi method for optimizing multi-response simulation problems*, Engineering Optimization, vol. 40, iss. 6, pp. 517-528, 2008, doi: [10.1080/03052150701857645](https://doi.org/10.1080/03052150701857645)
- [32] D. Ju-Long, *Control problems of grey systems*, System & control letters, vol. 1, iss. 5, pp. 288-294, 1982, doi: [10.1016/S0167-6911\(82\)80025-X](https://doi.org/10.1016/S0167-6911(82)80025-X)
- [33] M. Kumar, M.A. Megalingam, V. Baskaran, K.S. Hanumanth Ramji, *Effect of sliding distance on dry sliding tribological behaviour of Aluminium Hybrid Metal Matrix Composite (AlHMMC): An alternate for automobile brake rotor - A Grey Relational approach*, Proceedings of the Institution of Mechanical Engineers, Part J: Journal of Engineering Tribology, vol. 230, iss. 4, pp. 402-415, 2017, doi: [10.1177/1350650115602724](https://doi.org/10.1177/1350650115602724)
- [34] Y. Han, X. Liu, X. Bian, *In situ TiB<sub>2</sub> particulate reinforced near eutectic Al-Si alloy composites*,

- Composites: Part A, vol. 33, iss. 3, pp. 439-444, 2002, doi: [10.1016/S1359-835X\(01\)00124-5](https://doi.org/10.1016/S1359-835X(01)00124-5)
- [35] Y.P. Lim, S. Shamsuddin, M.H. Abdel, H.M.A. Megat Mohamad, *Grain refinement of LM6 Al-Si alloy sand castings to enhance mechanical properties*, Journal of Materials Processing Technology, vol. 162-163, pp. 435-441, 2005, doi: [10.1016/j.jmatprotec.2005.02.217](https://doi.org/10.1016/j.jmatprotec.2005.02.217)
- [36] Sudarshan, M.K. Surappa, *Dry sliding wear of fly ash particle reinforced A356 Al composites*, Wear, vol. 265, iss. 3-4, pp. 349-360, 2008, doi: [10.1016/j.wear.2007.11.009](https://doi.org/10.1016/j.wear.2007.11.009)
- [37] K.K. Alanemea, I.B. Akintundea, A.O. Peter, T.M. Adewalec, *Fabrication characteristics and mechanical behaviour of rice husk ash – Alumina reinforced Al-Mg-Si alloy matrix hybrid composites*, Journal of Materials Research and Technology, vol. 2, iss. 1, pp. 60-67, 2013, doi: [10.1016/j.jmrt.2013.03.012](https://doi.org/10.1016/j.jmrt.2013.03.012)
- [38] T. Nikps, B.O. Andrews, C. Cavallaro, *Mechanical Properties of Some Silicon Carbide Reinforced Aluminum Composites*, Journal of composite materials, vol. 21, iss. 5, pp. 481-492, 1987, doi: [10.1177/002199838702100505](https://doi.org/10.1177/002199838702100505)
- [39] F. Ferit, K. Sakip, *Microstructural characterization and wear properties of in situ AlB<sub>2</sub>-reinforced Al-4Cu metal matrix composite*, Journal of composite materials, vol. 50, iss. 12, pp. 1685-1696, 2015, doi: [10.1177/0021998315595709](https://doi.org/10.1177/0021998315595709)
- [40] A. Baradeswaran, A. Elaya Perumal, *Influence of B<sub>4</sub>C on the tribological and mechanical properties of Al 7075-B<sub>4</sub>C composites*, Composites: Part B, vol. 54, pp. 146-152, 2013, doi: [10.1016/j.compositesb.2013.05.012](https://doi.org/10.1016/j.compositesb.2013.05.012)
- [41] R.L. Deuis, C. Subramanian, J.M. Yellup, *Dry sliding wear of aluminium composites-a review*, Composites Science and Technology, vol. 57, iss. 4, pp. 415-435, 1997, doi: [10.1016/S0266-3538\(96\)00167-4](https://doi.org/10.1016/S0266-3538(96)00167-4)
- [42] M. Kok, K. Ozdin, *Wear resistance of aluminium alloy and its composites reinforced by Al<sub>2</sub>O<sub>3</sub> particles*, Journal of Materials Processing Technology, vol. 183, iss. 2-3, pp. 301-309, 2007, doi: [10.1016/j.jmatprotec.2006.10.021](https://doi.org/10.1016/j.jmatprotec.2006.10.021)
- [43] B.A. Kumar, N. Murugan, I. Dinaharan, *Dry sliding wear behavior of stir cast AA6061-T6/AlNp composite*, Transaction of Nonferrous Metal Society of China, vol. 24, iss. 9, pp. 2785-2795, 2014, doi: [10.1016/S1003-6326\(14\)63410-5](https://doi.org/10.1016/S1003-6326(14)63410-5)
- [44] A. Ravikiran, M.K. Surappa, *Effect of sliding speed on wear behaviour of A356 Al-30 wt.% SiC<sub>p</sub> MMC*, Wear, vol. 206, iss. 1-2, pp. 33-38, 1997, doi: [10.1016/S0043-1648\(96\)07341-3](https://doi.org/10.1016/S0043-1648(96)07341-3)
- [45] A. Halil, O. Yusuf, T. Mehmet, *Dry sliding wear behavior of in situ Al-Al<sub>4</sub>C<sub>3</sub> metal matrix composite produced by mechanical alloying technique*, Materials and Design, vol. 27, iss. 9, pp. 799-804, 2006, doi: [10.1016/j.matdes.2005.01.024](https://doi.org/10.1016/j.matdes.2005.01.024)
- [46] H. Mavros, A.E. Karantzalis, A. Lekatou, *Solidification observations and sliding wear behavior of cast TiC particulate-reinforced AlMgSi matrix composites*, Journal of composite materials, vol. 47, iss. 17, pp. 2149-2162, 2012, doi: [10.1177/0021998312454901](https://doi.org/10.1177/0021998312454901)
- [47] X.Y. Li, K.N. Tandon, *Microstructural characterization of mechanically mixed layer and wear debris in sliding wear of an Al alloy and an Al based composite*, Wear, vol. 245, iss. 1-2, pp. 148-161, 2000, doi: [10.1016/S0043-1648\(00\)00475-0](https://doi.org/10.1016/S0043-1648(00)00475-0)
- [48] S.C. Sharma, *The sliding wear behavior of Al6061-garnet particulate composites*, Wear, vol. 249, iss. 12, pp. 1036-1045, 2001, doi: [10.1016/S0043-1648\(01\)00810-9](https://doi.org/10.1016/S0043-1648(01)00810-9)